



Supplementary Materials for

High-fat diet–induced colonocyte dysfunction escalates microbiota-derived trimethylamine *N*-oxide

Woongjae Yoo *et al.*

Corresponding authors: Mariana X. Byndloss, mariana.x.byndloss@vumc.org; Andreas J. Bäumlner, jbaumlner@ucdavis.edu

Science **373**, 813 (2021)
DOI: 10.1126/science.aba3683

The PDF file includes:

Materials and Methods
Figs. S1 to S6
Tables S1 to S9
References

Other Supplementary Material for this manuscript includes the following:

MDAR Reproducibility Checklist

Materials and Methods

Animal Experiments

All experiments in this study were approved by the Institutional Animal Care and Use Committee (IACUC) at the University of California at Davis and by the IACUC at Vanderbilt University Medical Center.

Female mice do not respond as robustly to high-fat diet as male mice (31-33) and therefore the latter gender was chosen for this study. However, female mice feature increased hepatic flavin-containing monooxygenase activity compared to male mice (34). Male C57BL/6J Diet-Induced Obesity (DIO) (#380050) and Diet-Induced Obesity (DIO control) (#380056) mice, aged 16-17 weeks, were obtained from Jackson Laboratory. Germ-free Swiss Webster mice were bred and housed at the Division of Animal Care facility at Vanderbilt University Medical Center. Animals were either fed a 60% fat diet (HFD) (OpenSource Diets, #D12492) or a 10% fat control diet (LFD) (Open Source diets, #D12450J) from 5 weeks of age until the end of the experimental period (13-14 weeks total). For choline supplementation experiments, animals were kept on LFD or HFD from 5-15 weeks of age. Prior to experiments with conventional (C57BL/6J) mice, feces were cultured on MacConkey agar to ensure animals were *Enterobacteriaceae*-free. One week before the beginning of experiments, mice were switched to a 60% fat diet supplemented with 1% choline (HFD + 1% choline) (OpenSource Diets, #D19042202) or a 10% fat control diet supplemented with 1% choline (LFD + 1% choline) (Open Source diets, #D19042201) until the end of the experimental period (up to 5 weeks total). For 5-aminosalicylic acid (5-ASA) supplementation experiments, animals were kept on HFD or LFD from 5-15 weeks of age. One week before the beginning of experiments, mice were switched to a 60% fat diet supplemented with 1% choline (HFD + 1% choline) (OpenSource Diets, cat #: D19042202) or a 10% fat control diet supplemented with 1% choline (LFD + 1% choline) (Open Source diets, cat #: D19042201) or a 60% fat diet supplemented with 1% choline and 0.25% 5-ASA (Sigma-Aldrich #A3537) (HFD + 1% choline + 5-ASA) (OpenSource Diets, cat #: D20092103) or a 10% fat control diet supplemented with 1% choline + 0.25% 5-ASA (Sigma-Aldrich #A3537) (LFD + 1% choline) (Open Source diets, cat #: D20092102) until the end of the experimental period (up to 5 weeks total). In some experiments, drinking water was supplemented with 1mg/mL of aminoguanidine hydrochloride (Sigma-Aldrich #396494) for the duration of the experiment. In some Germ-free mouse experiments, mice were intragastrically inoculated with a defined microbiota (DM) community consisting of a mixture of 3×10^9 CFU of *Bacteroides thetaiotaomicron*, *Bacteroides caecimuris*, *Lactobacillus reuteri*, *Clostridium innocuum*, *Clostridioides mangenotti*, *Clostridium cochlearium* and *Clostridium sporogenes* (**Table S1**) at the start of the HFD + 1% choline or LFD + 1% choline treatment (one week before beginning of experiment). Body weights of mice

were collected at the beginning of each experiment. At day 0, depending on the experiment, mice were inoculated by intragastric gavage (1×10^9 CFU in 0.1 mL) with the indicated bacterial strains or strain mixtures in Luria-Bertani (LB) broth (BD Biosciences, #244620). *E. coli* Nissle 1917 was transformed with pCAL62 and strains YL219 and YL200 were transformed with plasmid pCAL61 to introduce a selectable marker. Dosage of bacterial strains administered to mice was confirmed by serial dilution and plating of the inoculum. Fecal colonization was determined by homogenizing fecal content in 1 mL of sterile PBS, followed by serial dilutions of the samples which were then plated in LB plates containing the appropriate antibiotics.

For colon length measurements, blood and plasma collection, histopathology analysis, hypoxia staining, and colonocyte isolation, mice were humanely euthanized by CO₂ administration at 17-21 weeks of age, and colonic tissue was collected as described below.

For long-term Enterobacteriaceae colonization studies, male C57BL/6J (Jackson Laboratory #000664) or C57BL6/NCrl (Charles River #027) mice aged 4 weeks, were obtained from The Jackson Laboratory or Charles River, respectively. Mice from The Jackson Laboratory mice were orally colonized with 1×10^9 CFU of the indicated individual *E. coli* strains in Luria-Bertani (LB) broth (BD Biosciences #244620). Mice from Charles River were not colonized as they have commensal Enterobacteriaceae in their gut microbiota. At 24 hours after oral colonization, fecal pellets were collected from each mouse and samples were then serially plated on MacConkey agar (BD Biosciences #DF0075073) plates to confirm *E. coli* and Enterobacteriaceae presence in the gut microbiota. After overnight incubation at 37°C, CFUs were calculated to obtain initial bacterial colonization levels for each experimental group. At 48 hours after colonization mice were placed on the indicated high-fat or low-fat diet for the duration of the experiment. Fecal pellets were collected weekly for 12 weeks and *E. coli* and Enterobacteriaceae fecal colonization was determined by homogenizing fecal content in 1 mL of sterile PBS, followed by serial dilutions of the samples which were then plated in MacConkey agar plates.

Bacterial culture conditions

The bacterial strains used in this study are listed in **Table S1**. *E. coli* strains were routinely grown aerobically at 37°C in LB broth (BD Biosciences #244620) or on LB plates. *Bacteroides thetaiotaomicron* and *Bacteroides caecimuris* were grown anaerobically at 37°C in mucin broth. *Lactobacillus reuteri* was grown anaerobically at 37°C in MRS broth (BD Biosciences #DF0881175). *Clostridium innocuum*, *Clostridioides mangenotti*, *Clostridium cochlearium* and *Clostridium sporogenes* were grown anaerobically at 37°C in Brain Heart Infusion (BHI) broth (BD Biosciences

#L4321843). When necessary, antibiotics were added to the media at the following concentrations: 0.1 mg/mL carbenicillin (Fisher BioReagents #BP26485), 0.05 mg/mL kanamycin (Sigma-Aldrich #25389-98-0), 0.03 mg/mL chloramphenicol (Alfa Aesar AAB2084122), or 0.05 mg/mL spectinomycin (Fisher BioReagents #BP29571).

For mucin broth preparation, porcine mucin (Sigma-Aldrich #M2378) was dissolved in No-Carbon E medium (NCE) (3.94 g/L monopotassium phosphate, 5.9 g/L dipotassium phosphate, 4.68 g/L ammonium sodium hydrogen phosphate tetrahydrate, 2.46 g/L magnesium sulfate heptahydrate) at a final concentration of 0.5 % (w/v). Mucin broth was sterilized by autoclave. Mucin broth was inoculated with a fresh colony of *Bacteroides* strains and incubated anaerobically for 72 hours at 37°C.

For bacterial growth on choline under microaerobic (1% oxygen) or anaerobic (0% oxygen) *in vitro* conditions, NCE minimal medium (28 mM KH₂PO₄, 28 mM K₂HPO₄·3H₂O and 16 mM NaNH₄HPO₄·4H₂O) supplemented with 1 mM MgSO₄, 0.1% Casamino acids and 1% vitamin and trace mineral solutions (American Type Culture Collection) was used. To evaluate the growth using choline as a sole carbon/energy source and nitrate as an alternative electron acceptor, 10 mM choline chloride (ACROS Organics #AC110290500), 10 mM glucose (ACROS Organics #AC410950010), 40 mM glycerol (Fisher Chemical #G334), 40 mM fumarate (Alfa Aesar #AAA1127622) and/or 40 mM sodium nitrate (Honeywell #6001504) were added into the medium. Indicated bacterial strains with 1×10^8 CFU were inoculated and incubated at 37°C in a hypoxia chamber (set at 1% oxygen) or in an anaerobic chamber (0% oxygen). 24 hours after inoculation, cultures were harvested, serially diluted with PBS and plated on the selective agar plates to enumerate the bacterial CFU. For *cutC* gene complementation, 10 mM arabinose was added into the medium to express CutC (Choline TMA-lyase) from the pWJ43 (pBAD18::*P*_{BAD}-*cutC*).

Generation of bacterial mutants

Primers and plasmids used to construct the bacterial strains in this study are listed in **Table S2** and **S3**. The phage λ -derived Red recombination system was used to delete genes in-frame. The Cm^R cassette from pKD3 plasmid was amplified using the *cutC*-Cm-F and *cutC*-Cm-R primers to construct WJ2 (*E. coli* MS 200-1 $\Delta cutC::Cm^R$), WJ270 (*E. coli* MS 200-1 $\Delta cutC::Cm^R \Delta cydA::Kan^R \Delta napA \Delta narG \Delta narZ$), WJ290 (*E. coli* MS 200-1 $\Delta cydA::Kan^R \Delta cutC::Cm^R$) and WJ299 (*E. coli* MS200-1 $\Delta cutC::Cm^R \Delta napA::Kan^R \Delta narG \Delta narZ$) mutants. The Kan^R cassette from pKD13 plasmid was amplified using the *cydA*-Kan-F and *cydA*-Kan-R or *napA*-Kan-F and *napA*-Kan-R primers to construct WJ39 (*E. coli* MS 200-1 $\Delta cydA::Kan^R$), WJ244 (*E. coli* MS 200-1 $\Delta cydA::Kan^R \Delta narG \Delta napA \Delta narZ$), WJ270 (*E. coli* MS 200-1 $\Delta cutC::Cm^R \Delta cydA::Kan^R \Delta napA \Delta narG \Delta narZ$), WJ290 (*E. coli* MS 200-1 $\Delta cutC::Cm^R \Delta napA::Kan^R \Delta narG \Delta narZ$), WJ137 (*E. coli* MS 200-1 $\Delta napA::Kan^R \Delta narG \Delta narZ$) and WJ299 (*E. coli* MS

200-1 $\Delta cutC::Cm^R \Delta napA::Kan^R \Delta narG \Delta narZ$) mutants, respectively. The following amplified PCR products were digested with DpnI (NEB #R0176S) and gel-purified. Electrocompetent cells of *E. coli* MS 200-1 carrying the Red recombinase expression plasmid pKD46 (Spec^R) were transformed with the desired PCR product. After transformation, recombinant bacteria containing the Cm^R or Kan^R cassette in place of the target genes were detected using chloramphenicol or kanamycin resistance and diagnostic PCR using primers flanking the targeted region. To construct the *E. coli* MS 200-1 $\Delta napA \Delta narG \Delta narZ$ triple deletion mutant, the upstream and downstream regions of approximately 0.5 kb flanking the *napA*, *narG* or *narZ* genes were amplified by PCR from the *E. coli* MS 200-1 genome. The pRDH10 suicide plasmid was digested with Sall (NEB #R3138S) and assembled with the fragments of each gene using the Gibson Assembly Master Mix (NEB #E2611S) to form plasmid pWJ45 (pRDH10::*ΔnarG*), pWJ46 (pRDH10::*ΔnapA*) or pWJ47 (pRDH10::*ΔnarZ*). pWJ45 was transformed into *E. coli* S17-1 λpir and conjugated into *E. coli* MS 200-1 using *E. coli* S17-1 λpir as the donor strain. Clones that had integrated the suicide plasmid were subjected to sucrose counter-selection and a colony that was sucrose resistant and Cm^S was verified by PCR to be *E. coli* MS 200-1 $\Delta narG$ mutant. Then, Plasmid pWJ46 was transformed into *E. coli* S17-1 λpir and conjugated into *E. coli* MS 200-1 $\Delta narG$ mutant using *E. coli* S17-1 λpir as the donor strain. Clones that had integrated the suicide plasmid were subjected to sucrose counter-selection and a colony that was sucrose resistant and Cm^S was verified by PCR to be *E. coli* MS 200-1 $\Delta napA \Delta narG$ mutant. Then, Plasmid pWJ47 was transformed into *E. coli* S17-1 λpir and conjugated into *E. coli* MS 200-1 $\Delta napA \Delta narG$ mutant using *E. coli* S17-1 λpir as the donor strain. Clones that had integrated the suicide plasmid were subjected to sucrose counter-selection and a colony that was sucrose resistant and Cm^S was verified by PCR to be *E. coli* MS 200-1 $\Delta napA \Delta narG \Delta narZ$ mutant.

Plasmid construction for *cutC* gene complementation

For the complementation of WJ2 (*E. coli* MS 200-1 $\Delta cutC::Cm^R$), the *cutC* gene was PCR amplified using primers cutC-comple-F and cutC-comple-R (**Table S2**). The PCR fragments were gel purified and cloned into Sall digested pBAD18 (Kan^R) using Gibson Assembly Master Mix (NEB #E2611S). The resulting plasmid pWJ43 (pBAD18::PBAD-*cutC*) was transformed into the strain WJ2 (*E. coli* MS 200-1 $\Delta cutC::Cm^R$) for *cutC* gene complementation.

E. coli* gene expression *in vitro

To determine bacterial gene expression *in vitro*, NCE minimal medium (28 mM KH₂PO₄, 28 mM K₂HPO₄·3H₂O and 16 mM NaNH₄HPO₄·4H₂O) supplemented with 1 mM MgSO₄, 0.1% Casamino acids (Fisher BioReagents #BP1424), and 1% vitamin (ATCC

#MD-VS) and trace mineral solutions (ATCC #MD-TMS) was inoculated with 1×10^8 CFU of *E. coli* MS 200-1 strains and cultured at 37°C under microaerobic (1% oxygen) or anaerobic condition. 10 mM choline chloride (ACROS Organics #AC110290500) and 40 mM sodium nitrate (Honeywell #6001504) were provided as a sole carbon/energy source and an alternative electron acceptor into the medium respectively. Total RNA was extracted from the bacterial cells grown to the different time point (mid-log phase) (1% oxygen at 8 hour p.i. or anaerobic at 16 hour p.i.) using Total RNA Purification Plus Kit (Norgen, #48300). cDNA was generated by iScript gDNA Clear cDNA Synthesis Kit (Bio-Rad #1725035). Real-time PCR was performed using iQ SYBR Green Supermix (Bio-Rad #1708882) and primers described on **Table S4**. Data was acquired in a CFX384 Real-Time System (Bio-Rad) and analyzed using the comparative Ct method. Target gene transcription of each sample was normalized to *GyrB* mRNA levels.

Detection of *cutC* by degenerate PCR

Degenerate primers were designed based on an alignment from 85 *cutC* sequences from different species. These primers amplify a 314-bp conserved portion of the *cutC* gene. Primer sequences were 5'-TTYGCIGGITAYCARCCNTT-3' (dPCR-cutC-F) and 5'-TGNGGRTCIACYCAICCCAT-3' (dPCR-cutC-R) (*I*). This primer set was used to amplify *cutC* gene from genomic DNA isolated from cultures of *E. coli* MS 200-1, *Bacteroides thetaiotaomicron*, *Bacteroides caecimuris*, *Limosilactobacillus reuteri*, *Clostridium innocuum*, *Clostridioides mangenotti*, *Clostridium cochlearium* and *Clostridium sporogenes*. PCRs were analyzed by agarose gel electrophoresis stained with SYBR Safe Stain (Invitrogen #S33100).

Real-time PCR for *cutC* detection

Quantification of the *cutC* gene copy number in the microbiota was performed by Real-time PCR using the degenerate *cutC* primers described above. Bacterial DNA was isolated from feces of mice fed a HFD + 1% choline or a LFD + 1% choline before and after *E. coli* MS200-1 wild-type infection. Real-time PCR was performed using iQ SYBR Green Supermix (Bio-Rad #1708882) and analyzed using the comparative Ct method. *cutC* gene levels of each sample was normalized to *Eubacteria* specific primer set. *Eubacteria* primer sequences were 5'-ACTCCTACGGGAGGCAGCAGT-3' (Eubacteria-F) and 5'-ATTACCGCGGCTGCTGGC-3' (Eubacteria-R).

Palmitate preparation

Palmitate stock solution containing 100 mM palmitate acid was prepared by dissolving palmitic acid (Sigma Aldrich #NC1064170) in 0.1 M NaOH at 70°C for 1 hour. 100 mM palmitate was then diluted to 50 mM in 5% fatty acid free bovine serum albumin (BSA) (MPBiomedicals #AAJ6578822). Stock stored at -20°C and heated to 55°C prior to experiments.

Caco-2 cells culture

Caco-2 cells (ATCC #HTB-37) were grown in Minimal Essential Media (MEM) (Gibco #11090081), 10% Fetal Bovine Serum (Gibco #16140071), 1% Glutamax (Gibco #35030061), 1% MEM Nonessential Amino Acids (Corning #11140050), and 1% Sodium Pyruvate (Gibco #11360070) at 37°C and 5% CO₂.

Caco-2 cells RNA isolation and Quantitative real-time PCR

Cells were grown until 70% confluency and then seeded into 6 well plates. After 48 hours, 2 mM butyrate (Sigma Aldrich #AC263191000) and 25 mM HEPES (Gibco #15630080) were added to cells. Butyrate treatment was repeated every 48 hours for 7 days to ensure full epithelial differentiation. On day 7, palmitate (2.5 mM) or fatty acid free BSA control was added to differentiated cells followed by 24 hr incubation at 37°C and 5% CO₂. After incubation, cells were washed with DPBS (Gibco #14190144), 0.05% Trypsin-EDTA (Gibco #25300054) was added, and cells harvested. Cell pellets were stored at -80°C until further use. RNA from palmitate treated caco-2 cells was isolated using Total RNA Purification Plus Micro kit according to manufacturer's protocol (Norgen Biotek Corporation #NC1304915) and stored at -80°C. RNA was reverse transcribed using iScript gDNA Clear cDNA Synthesis Kit (Bio-Rad #1725035). Quantitative PCR was performed using iQ SYBR Green Supermix (Bio-Rad #1708882) and the appropriate primer sets (**Table S5**). Expression of target genes was normalized to the house keeping gene 18S.

Caco-2 cells measurement of ATP production rates

Experiments were performed using the Real-Time ATP Rate Assay kit (Agilent #103592-100) according to the manufacturer's instructions and carried out using an Agilent Seahorse XFe96 Analyzer. Fourteen days prior to palmitate treatment, Caco-2 cells were seeded to confluency in an XF Cell Culture Microplate (Agilent #102416-100) and placed in a tissue culture incubator at 37°C. Cell culture media was replaced every two days. 24 hr prior to completing the assay, cells were treated with palmitate (0.5, 1.0, 1.5 or 2.5 mM) or fatty acid free BSA control. One day prior to the assay, a Utility Plate (Agilent #102416-100) was hydrated with tissue culture grade water at 37°C in a non-CO₂ incubator. Immediately prior to completing the assay, water was removed from the Utility Plate and replaced with 200 µL of pre-warmed, 37°C XF Calibrant (Agilent #100840-000) and placed in a non-CO₂ incubator for 45 min to 1 hour. Also, immediately prior to completing the assay, spent culture medium was replaced with 180 µL Seahorse XF DMEM Medium, pH 7.4 (Agilent #103575-100) supplemented with 5.5 mM glucose (Agilent #103577-100), 1% GlutaMAX-I (Gibco #35050061), and 1 mM sodium pyruvate (Gibco #11360070) (hereon referred to as Agilent Complete Medium), and cells were placed in a non-CO₂ incubator at 37°C for 1 hour. Stock compounds were prepared

and loaded into the Sensor Cartridge (Agilent) ports according to the manufacturer's instructions, maintaining a final well concentration of 1.5 μ M oligomycin and 0.5 μ M rotenone/antimycin A.

Colonocyte isolation

The proximal colon was flushed with ice-cold phosphate buffered saline (PBS) (Gibco #14190144) using a 10 mL syringe fitted with an 18-gauge blunt needle before opening lengthwise, cutting into 2-4 cm pieces and placing in a 15 mL conical centrifuge tube filled with 10 mL ice-cold PBS (Gibco #14190144) on ice. Tubes were gently inverted four times, PBS (Gibco #14190144) wash was removed and replaced with additional ice-cold PBS (Gibco #14190144) before transfer to sterile petri dishes where colon tissue was cut into <5 mm pieces using a razor blade. Tissue pieces were placed in a 15 mL conical centrifuge tube dissociation reagent #1 (30 mM EDTA, 1.5 mM DTT, pH 8 in PBS) and incubated for 20 minutes buried in ice. Then, Tissue pieces were transferred to a new 15 mL conical centrifuge tube containing pre-warmed (37°C) dissociation reagent #2 (30 mM EDTA, pH 8 in PBS) and samples were incubated at 37°C for 10 min. After incubation, tubes containing the samples were shaken vigorously for 30 seconds to release epithelium from the basement membrane. Cell suspension was transferred to a new 15 mL conical centrifuge tube, leaving any large remnant colon tissue, and cells were pelleted by centrifugation at 800 x g for 5 minutes at 4°C. Supernatant was removed and the cell pellet was resuspended in 1 mL TRIzol method (Invitrogen #15596018) for subsequent RNA extraction, or it was flash frozen in liquid nitrogen for subsequent lactate, ATP or PDH activity measurements.

Primary mouse colonocyte RNA isolation and Quantitative real-time PCR

Colonocyte RNA was isolated by the TRIzol method (Invitrogen #15596018). following manufacturer's protocol. RNA was reverse transcribed using iScript gDNA Clear cDNA Synthesis Kit (Bio-Rad #1725035). Quantitative PCR was performed using iQ SYBR Green Supermix (Bio-Rad #1708882) and the appropriate primer sets (**Table S6**).

Histopathology analysis

Colonic tissue was fixed in 10% phosphate-buffered formalin, paraffin-embedded and 5 μ m sections of tissue were stained with hematoxylin and eosin. Scoring of blinded tissue sections was performed by a veterinary pathologist based on the criteria listed in **Table S7**. Representative images were taken using a Leica DM750 microscope and a Leica ICC50W camera.

Alcian blue staining

Colonic tissue was fixed in 10% phosphate-buffered formalin paraffin-embedded and 5 μ m sections of tissue were stained with alcian blue staining by the UC Davis VMTH

Histopathology laboratory. Scoring of blinded tissue sections was performed by a veterinary pathologist based on the criteria listed in **Table S8**. Representative images were taken using a Leica DM750 microscope and a Leica ICC50W camera.

Hypoxia staining

For detection of hypoxia, mice were treated with 60mg/kg of pimonidazole HCl i.p. (HypoxyprobeTM-1 kit, Hypoxyprobe #HP1-200kit) one hour prior to euthanasia. Colon samples were fixed in 10% buffered formalin and paraffin-embedded tissue was probed with mouse anti- pimonidazole monoclonal IgG1 (MAb 4.3.11.3) and then stained with Alexa fluor 546-conjugated goat anti- mouse IgG antibody (Life Technologies #A1103). Samples were counterstained with DAPI using SlowFade Gold mountant (Invitrogen #S36936). Samples were scored based on the degree of colonic epithelial hypoxia (0: no hypoxia; 1: mild focal hypoxia; 2: moderate multifocal hypoxia; 3: intense diffuse hypoxia) Representative images were obtained using either a Zeiss Axiovert 200 M fluorescent microscope or a Zeiss LSM 880 confocal microscope, and brightness adjusted using either Adobe Photoshop CS2 or ImageJ.

ATP measurements

For determination of intracellular ATP measurements, primary colonocytes were isolated as described above. ATP measurement in colonocyte lysates was performed by using a ATP Colorimetry Assay Kit (Biovision #K354), according to manufacturer's instructions.

PDH activity measurements

Colonocytes were extracted and flash frozen at indicated time points. To measure PDH activity, colonocytes were lysed with RIPA buffer and spun down at RT for 5 minutes at 13,000 rpm to remove cellular debris. PDH activity was measured in supernatants by using the PDH activity assay kit (BioVision #K679) according to the manufacturer's instructions.

Nitrate measurements

Intestinal nitrate measurements were performed as described previously (14). Briefly, mice were euthanized, and the intestine was removed and divided along its sagittal plane. The mucus layer was gently scraped from the tissue and homogenized in 200 μ L PBS and then placed on ice. Samples were centrifuged at $5,000 \times g$ for 10 min at 4°C to remove the remaining solid particles. The supernatant was then filter sterilized (0.2- μ m Acrodisc syringe filter, Pall Life Sciences). Measurement of intestinal nitrate followed an adaptation of the Griess assay. In this study, nitrate was first reduced to nitrite by combining 50 μ L of each sample with 50 μ L of Griess reagent 1 containing vanadium(III) chloride (0.5 M HCl, 0.2 mM VC1₃, 1% sulfanilamide), and then the mixture was incubated at room temperature for 10 min. Next, 50 μ L of Griess reagent 2

[0.1% (1-naphthyl)ethylenediamine dichloride] was added to each sample. Absorbance at 540 nm was measured immediately after the addition of Griess reagent 2 to detect any nitrite present in the samples. The samples were then incubated for 8 hours at room temperature (to allow for reduction of nitrate to nitrite), and the absorbance at 540 nm was measured again. The initial absorbance (prior to reducing nitrate to nitrite) was subtracted from the absorbance after 8 hours to determine nitrate concentrations in the cecal mucus layer. Samples were tested in duplicate, and all measurements were standardized to the initial sample weight.

TMAO measurements

Plasma trimethylamine N-oxide (TMAO) was quantified using liquid chromatography–mass spectrometry (LC-MS) methods described by Wang et al. [Anal. Biochem, 2014] with minor modifications. TMAO (Sigma-Aldrich) standards ranging from 0 μM to 100 μM of non-deuterated analytes in 100% Methanol were run in order to establish analyte standard curves. Two-fold serial dilutions of a 100 μM stock solution in methanol was used to make 13 standards. 10 μM of surrogate standard (SSTD) were prepared comprising of deuterated analytes in Methanol. All reagent solvents were mass spectrometry grade and purchased from Fisher Scientific (Waltham, Mass.). Briefly, samples (20 μL plasma) were aliquoted to a 2 mL Eppendorf tube and mixed with 80 μL of 10 μM surrogate standard. Samples were vortexed for 30 seconds and centrifuged at 18,000 g at 10°C for 10 min. Supernatant was transferred to 150 μL glass inserts in High Performance Liquid Chromatography (HPLC) vials. To prepare standards for sample quantification, 80 μL of 10 μM SSTD and 20 μL of each standard were aliquoted directly to the glass inserts in HPLC vials and briefly vortexed. Analytes were monitored using electrospray ionization in positive-ion mode with multiple reaction monitoring (MRM) of precursor and characteristic production transitions as shown in **Table S9**. The parameters for the ion monitoring were as follows: spray voltage, 4.5 kV; curtain gas, 15; GS1, 60; GS2, 50; CAD gas, medium; Nitrogen (99.95% purity) was used as the source and collision gas. Integration and quantification of values was done using Analyst 1.6.2 software. Standard linearity was calculated using linear regression model.

Quantification and statistical analysis. Fold changes of ratios (bacterial competitive index and mRNA levels), and bacterial numbers were transformed logarithmically prior to statistical analysis. An unpaired Student's t test was used on the transformed data to determine whether differences between groups were statistically significant ($p < 0.05$). When more than two treatments were used, statistically significant differences between groups were determined by one-way ANOVA followed by Tukey's HSD test (between > 2 groups). Significance of differences in histopathology, alcian blue or hypoxia scores was determined by a one-tailed non- parametric test (Mann-Whitney).

Fig. S1

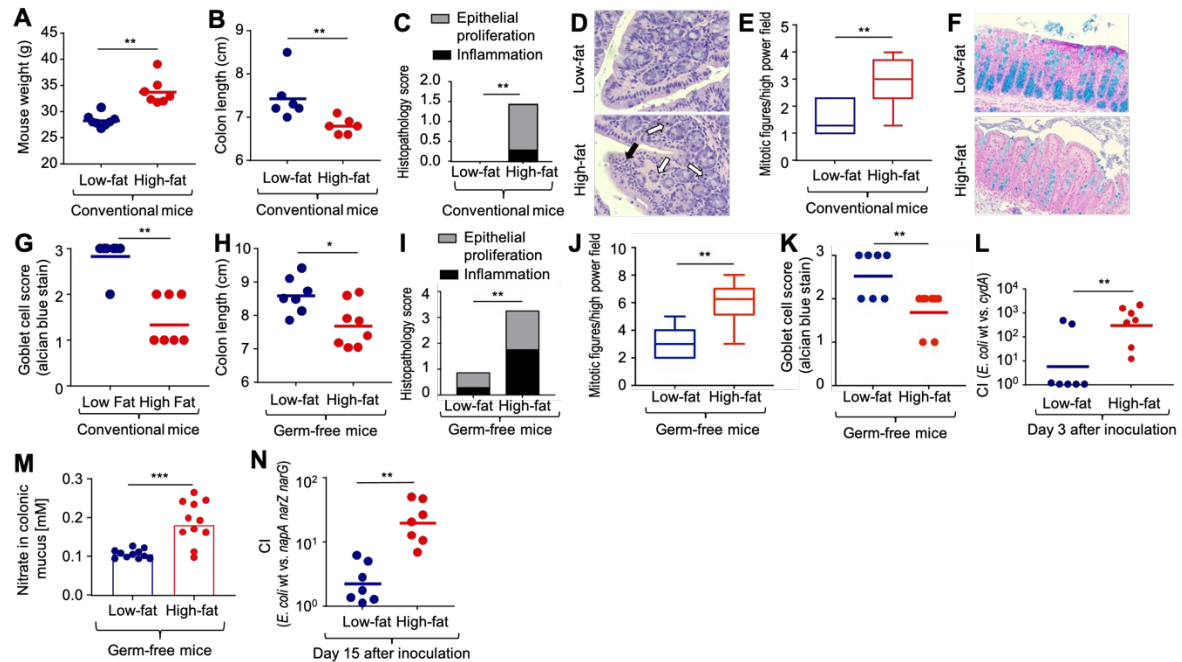


Figure S1: High-fat diet induces low-grade mucosal inflammation. (A-G, L and N) Conventional (C57BL/6J) mice were reared and maintained on a low-fat diet or a high-fat diet. Mouse body weight (A) and colon length (B) were determined during necropsy. (C-E) A veterinary pathologist scored histopathological changes in blinded sections of the cecum. Histopathology score (C) and representative images (D) are shown. Black arrow indicates metaplasia and open arrows indicate mitotic figures. (E) The frequency of mitotic figures was scored in blinded sections. (F and G) Goblet cells were visualized histologically by Alcian Blue (Mucin Stain) staining, which is specific for sulfated and carboxylated acid mucopolysaccharides and sulfated and carboxylated sialomucins. Representative images (F) and a quantification of the number of goblet cells (G) are shown. (H-K and M) Germ-free (Swiss-Webster) mice were reared and maintained on a low-fat diet or a high-fat diet. (H) Colon length was determined during necropsy. (I-K) A veterinary pathologist scored histopathological changes (I), mitotic figures (J) and goblet cells visualized by Alcian Blue staining (K) in blinded sections of the cecum. (L) Mice were inoculated with a 1:1 mixture of *E. coli* strain Nissle 1917 (wt) and an isogenic *cydAB* mutant and CFU were determined at the indicated time point to calculate the competitive index (CI). (M) Nitrate concentrations were determined in colonic mucus. (N) Mice were inoculated with a 1:1 mixture of *E. coli* strain Nissle 1917 (wt) and an isogenic *napA narG narZ* mutant and CFU were determined at the indicated time point to calculate the CI. (A, B, G, H and K-L) Each dot represents data from one animal (biological replicate). (C, E, I, J) N=7 biological replicates. *, P<0.05; **, P<0.01; ***, P<0.001 using unpaired two-tailed Student's t-test (A-B, E, H, J, L-N) or one-tailed Mann-Whitney test (C, G, I, K).

Fig. S2

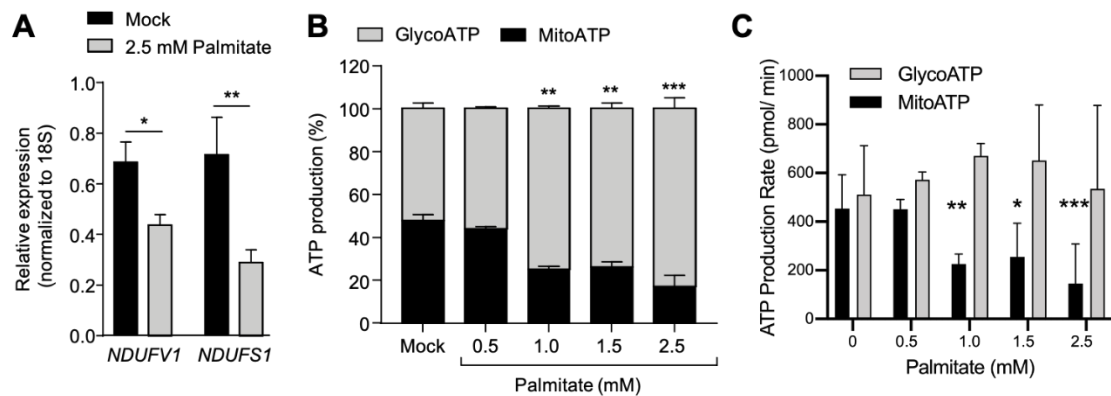


Figure S2: Palmitate impairs mitochondrial bioenergetics in cultured human colonic epithelial cancer (Caco-2) cells. Caco-2 cells were treated with indicated concentrations of palmitate for 24 hours. (A) Changes in the expression of genes encoding NADH:ubiquinone oxidoreductase core subunit V1 (*NDUFV1*) and NADH:ubiquinone oxidoreductase core subunit S1 (*NDUFS1*) were determined by quantitative real-time PCR. Bars represent geometric means \pm geometric error. (B-C) Relative (B) and absolute (C) ATP production rates coming from oxidative phosphorylation in the mitochondria (MitoATP) or substrate level phosphorylation by glycolysis (GlycoATP) were determined using Agilent Seahorse XF. Statistical difference between ATP coming from mitochondria versus glycolysis are indicated. (A) $N = 6$ biological replicates (average of triplicate technical replicate per biological replicate). (B,C) $N = 12$ biological replicates (average of triplicate technical replicate per biological replicate). *, $P < 0.05$; **, $P < 0.01$; ***, $P < 0.001$ using paired two-tailed Student's t-test.

Fig. S3

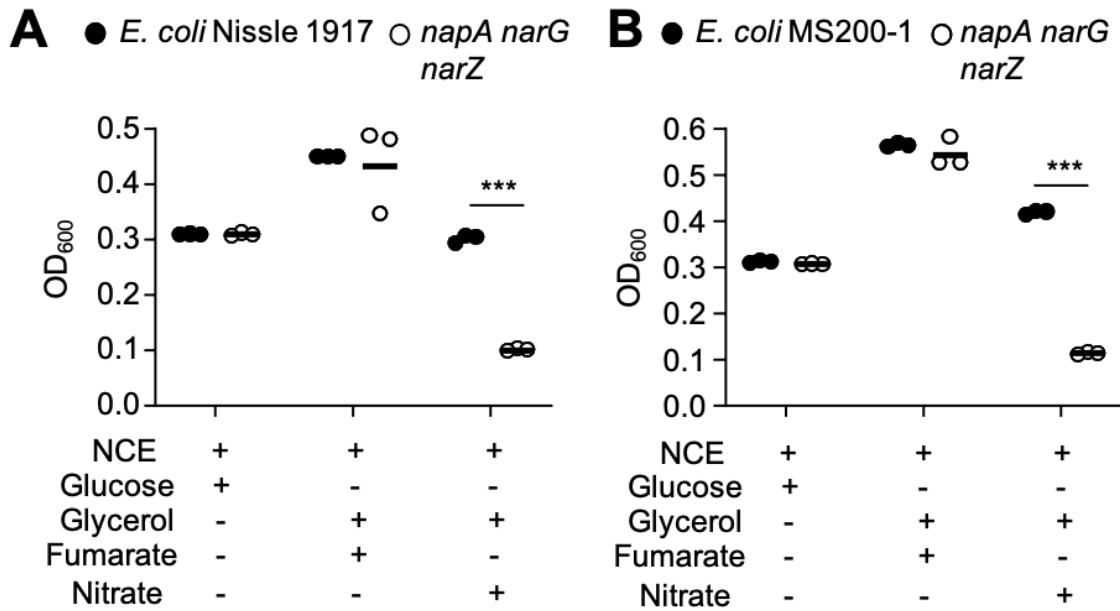


Figure S3: Characterization of *E. coli* mutants deficient for nitrate respiration for anaerobic growth *in vitro*. (A and B) The indicated *E. coli* Nissle 1917 (A) or MS200-1 strains (B) were grown anaerobically in no-carbon essential (NCE) medium supplemented with the indicated carbon sources and electron acceptors. Each dot represents one biological replicate (average of duplicate technical replicate per biological replicate). ***, $P < 0.001$ using unpaired two-tailed Student's t-test.

Fig. S4

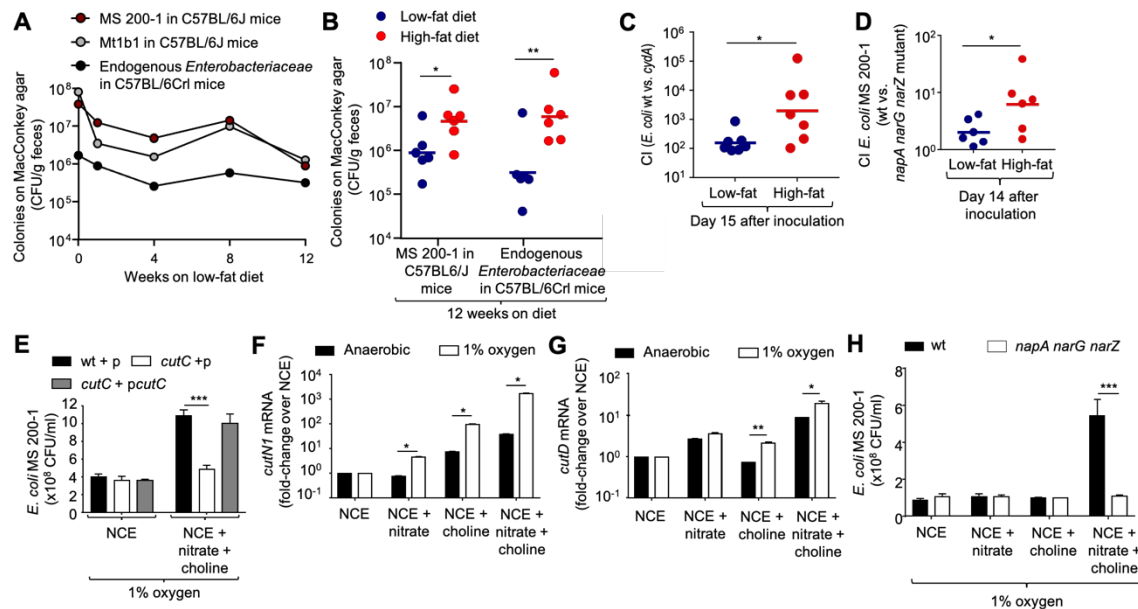


Figure S4: Effect of respiratory electron acceptors on growth of *E. coli* MS 200-1. (A-D) Mice were reared and maintained on a low-fat diet or a high-fat diet. (A) C57BL/6J mice from Jackson laboratories were inoculated with *E. coli* strains MS 200-1 or Mt1b1 and compared to C57BL/6Crl mice from Charles River laboratories that carry endogenous *Enterobacteriaceae*. Colony-forming units (CFU) in the feces were determined using selective MacConkey agar at the indicated time points after starting low-fat diet. (B) C57BL/6J mice from Jackson laboratories inoculated with *E. coli* strains MS 200-1 or C57BL/6Crl mice from Charles River laboratories were maintained on a high-fat diet or a low-fat diet. CFU in the feces were determined using selective MacConkey agar. (C) Mice were inoculated with a 1:1 mixture of *E. coli* MS 200-1 (wt) and an isogenic *cydA* mutant and CFU were determined at the indicated time point to calculate the competitive index. (D) Mice were inoculated with a 1:1 mixture of *E. coli* MS 200-1 (wt) and an isogenic *napA narG narZ* mutant and CFU were determined at the indicated time point to calculate the competitive index. (E) *In vitro* growth in a hypoxia chamber with 1% oxygen of *E. coli* MS 200-1 carrying a cloning vector (wt+p), a *cutC* mutant carrying a cloning vector (*cutC*+p) and a *cutC* mutant complemented with the cloned *cutC* gene (*cutC*+*pcutC*) in non-carbon essential (NCE) medium supplemented with the indicated nutrients. (F and G) Expression of *cutN1* (F) and *cutD* (G) was determined by quantitative real-time PCR in RNA isolated from *E. coli* MS 200-1 grown under the indicated conditions. (H) *In vitro* growth in a hypoxia chamber of *E. coli* MS 200-1 (wt) and an isogenic *napA narG narZ* mutant in NCE medium supplemented with the indicated nutrients. (B-D) Each dot represents data from one animal (biological replicate). (E-H) N=4 biological replicates (average of triplicate technical replicate per biological replicate). Bars represent geometric

means \pm geometric error. *, P<0.05; **, P<0.01; ***, P<0.001 using unpaired two-tailed Student's t-test (B-D, F-H) or one-way ANOVA followed by Tukey's HSD test (E).

Fig. S5

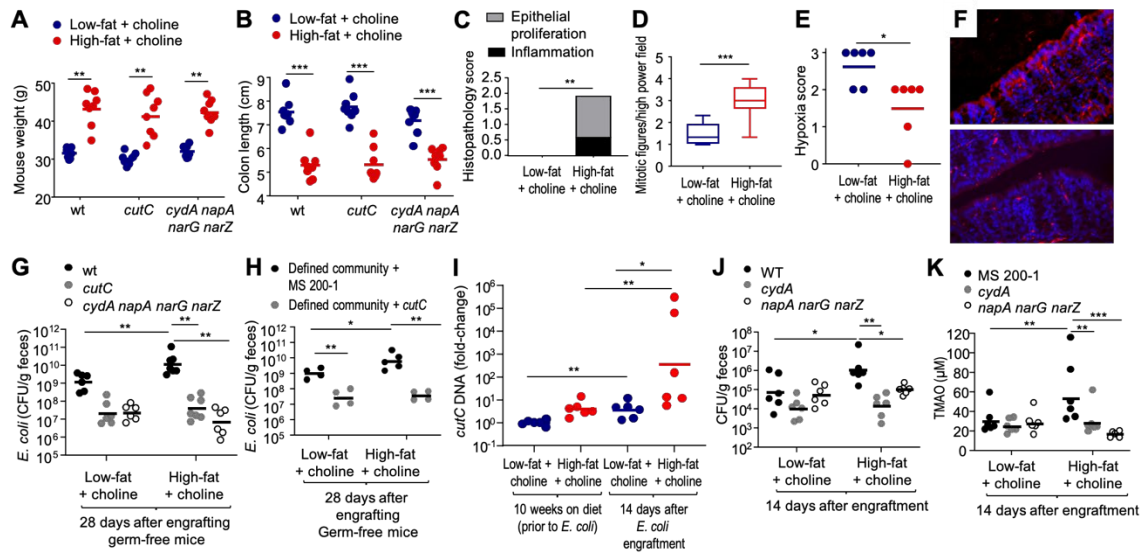


Figure S5: High-fat diet escalates *E. coli* choline metabolism. Conventional (C57BL/6J) mice were reared and maintained on a choline-supplemented low-fat diet or a choline-supplemented high-fat diet. (A and B) Mice were inoculated with *E. coli* MS 200-1 (wt), an isogenic *cutC* mutant or an isogenic *cydA napA narG narZ* mutant. Mouse body weight (A) and colon length (B) were determined during necropsy. (C-F) A veterinary pathologist scored histopathological changes in blinded sections of the cecum. Histopathology score (C) and scoring of mitotic figures (D) are shown. (E and F) Mice were injected with pimonidazole one hour before euthanasia. Binding of pimonidazole was detected using hypoxyprobe-1 primary antibody and a Cy-3 conjugated goat anti-mouse secondary antibody (red fluorescence) in the sections of proximal colon that were counterstained with DAPI nuclear stain (blue fluorescence). Hypoxia score (E) and representative images (F) are shown. (G) Germ-free (Swiss Webster) mice were mono-associated with the indicated *E. coli* strains and colony-forming units in the feces were determined 28 days later. (H) Germ-free (Swiss Webster) mice were engrafted with a defined microbial community containing either *E. coli* strain MS 200-1 or an isogenic *cutC* mutant and colony-forming units in the feces were determined 28 days later. (I) Conventional (C57BL/6J) mice were maintained for 10 weeks on a choline supplemented low-fat or high-fat diet and feces were collected for analysis. Mice were then inoculated with *E. coli* strain MS 200-1, maintained on the same diet and feces was collected for analysis 14 days later. Quantification of *cutC* DNA copy numbers in the microbiota was performed by quantitative real-time PCR with degenerate primers. The graph shows fold-change in *cutC* copy number over feces from mice on a low-fat diet prior to *E. coli* engraftment. (J and K) Conventional (C57BL/6J) mice were engrafted with the indicated *E. coli* MS 200-1 strains and maintained on choline-supplemented low-fat or high-fat diet. (J) *E. coli* was enumerated in the feces 14 days after engraftment. (K) TMAO levels in the plasma were determined 14 days after engraftment.

(A, B, G, H and G-I) Each dot represents data from one animal (biological replicate). (C-D) $N = 6$ biological replicates. *, $P < 0.05$; **, $P < 0.01$; ***, $P < 0.001$ using unpaired two-tailed Student's t-test (A-B, D, H-I), or one-tailed Mann-Whitney test (C, E) or one-way ANOVA followed by Tukey's HSD test (G, J-K).

Fig. S6

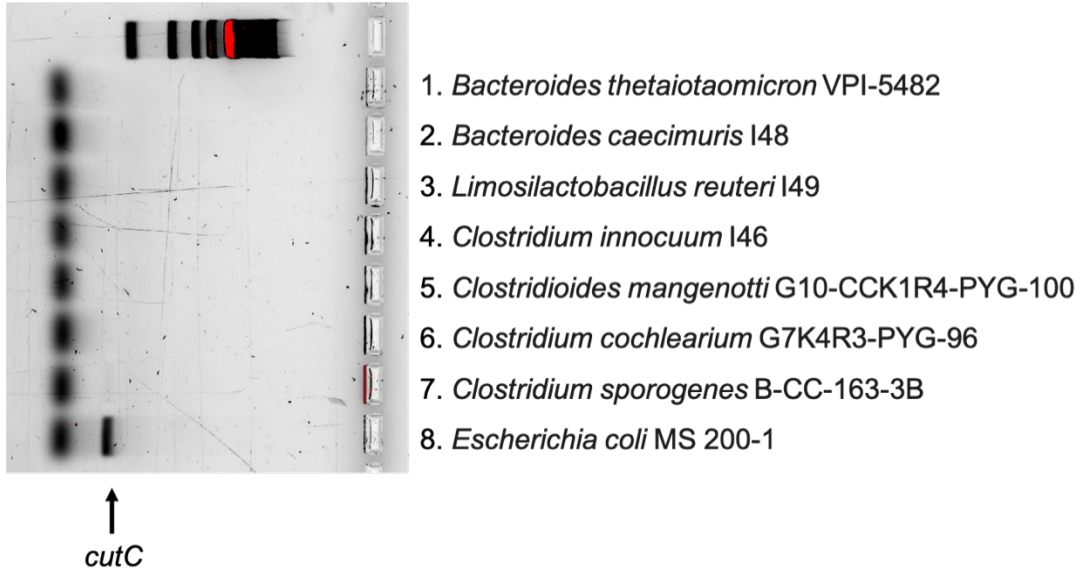


Figure S6: Detection of *cutC* in strains of the defined microbial community by degenerate PCR. Degenerate primers that amplify a 314-bp conserved portion of the *cutC* gene (*I*) were used to detect the presence of the gene in genomic DNA isolated from cultures of the indicated bacterial strains.

Table S1. Bacterial strains used in this study

Name	Description	Reference/ source
<i>E. coli</i> Nissle 1917	<i>E. coli</i> isolated from the feces of a healthy volunteer by Dr. Nissle in 1917	(16)
CAL222	<i>E. coli</i> Nissle 1917 $\Delta napA \Delta narG \Delta narZ::Kan^R$	(35)
YL219	<i>E. coli</i> Nissle 1917 $\Delta cydAB$	(14)
YL200	<i>E. coli</i> Nissle $\Delta napA \Delta narG \Delta narZ \Delta cydAB$	(14)
<i>E. coli</i> MS 200-1	<i>E. coli</i> wild type isolate MS 200-1	(26)
<i>E. coli</i> S17-1 λpir	C600::RP4 2-(Tet::Mu) (Kan::Tn7) $\lambda pir recA1 thi pro hsdR (r^m^+)$	(36)
WJ2	<i>E. coli</i> MS 200-1 $\Delta cutC::Cm^R$	This study
WJ39	<i>E. coli</i> MS 200-1 $\Delta cydA::Kan^R$	This study
WJ80	<i>E. coli</i> MS 200-1 $\Delta napA \Delta narG \Delta narZ$	This study
WJ137	<i>E. coli</i> MS 200-1 $\Delta napA::Kan^R \Delta narG \Delta narZ$	This study
WJ244	<i>E. coli</i> MS 200-1 $\Delta cydA::Kan^R \Delta napA \Delta narG \Delta narZ$	This study
WJ270	<i>E. coli</i> MS 200-1 $\Delta cutC::Cm^R/\Delta cydA::Kan^R \Delta napA \Delta narG \Delta narZ$	This study
WJ290	<i>E. coli</i> MS 200-1 $\Delta cydA::Kan^R \Delta cutC::Cm^R$	This study
WJ299	<i>E. coli</i> MS 200-1 $\Delta cutC::Cm^R \Delta napA::Kan^R \Delta narG \Delta narZ$	This study
<i>E. coli</i> Mt1b1	<i>E. coli</i> isolated from feces of a healthy mouse	DSMZ
VPI-5482	<i>Bacteroides thetaiotaomicron</i>	(37)
I48	<i>Bacteroides caecimuris</i>	DSMZ
I49	<i>Limosilactobacillus reuteri</i>	DSMZ
I46	<i>Clostridium innocuum</i>	DSMZ
G10-CCK1R4-PYG-100	<i>Clostridioides mangenotti</i>	DSMZ
G7K4R3-PYG-96	<i>Clostridium cochlearium</i>	DSMZ
B-CC-163-3B	<i>Clostridium sporogenes</i>	DSMZ

Table S2. Primers for bacterial mutant and plasmid construction used in this study

Name	Sequence (5' -> 3')	References
cutC-Cm-F	5'-GTTTTAAAGAGGCTTGCCAGGCATTTTATCTGTT CCAGTTTGTAGGCTGGAGCTGCTTCG-3'	This study
cutC-Cm-R	5'-TTATCTTCGTAAACCAGTTTGC GGATGGCCGCC ATTGAATATATGAATATCCTCCTTAGTTC-3'	This study
cutC-comple-F	5'-CTTGCATGCCTGCAGTCCGGTTGCGATCCGTCT TA-3'	This study
cutC-comple-R	5'-GGGGATCCTCTAGAGCTTTATCGCCAGGCCTGG AG-3'	This study
cydA-Kan-F	5'-GGGTTCACTCTCGGAGTCTTCATGCGATGAGCA AGGAGTCTGTAGGCTGGAGCTGCTTCG-3'	This study
cydA-Kan-R	5'-CCGATAACTGGAGTATCCACGGAACGCGTTGCA ATGATGCATTCCGGGGATCCGTCGACC-3'	This study
napA-Kan-F	5'-TGCTGAATATACGCTGGAAAAACCGCCGAAAT GACCGGCTGTAGGCTGGAGCTGCTTCG-3'	This study
napA-Kan-R	5'-TCTTCAGTTTTGAAGCGGCGGAGAACTGGACT AACTGCCATTCCGGGGATCCGTCGACC-3'	This study
napA-del-F1	5'-TCTCAAGGGCATCGTGGCGTCGGCAGTAGTTGG C-3'	This study
napA-del-R1	5'-ACTAACTGCCGCCGGTCATTTCCGGCGGTTT-3'	This study
napA-del-F2	5'-AATGACCGGCGGCAGTTAGTCCAGTTCTCC-3'	This study
napA-del-R2	5'-GCATAAGGGAGAGCGGTGCCAGTGCTCCAGGA CGC-3'	This study
narG-del-F1	5'-TCTCAAGGGCATCGACTACGCTGCGGGTCGTAT G-3'	This study
narG-del-R1	5'-TTTTTCCAGTAGAAACGCCGGTAATCTGCT-3'	This study
narG-del-F2	5'-CGGCGTTTCTACTGGAAAAAGGCGAATGC-3'	This study
narG-del-R2	5'-GCATAAGGGAGAGCGCGGGATCAGCTCGTGAA CGT-3'	This study
narZ-del-F1	5'-TCTCAAGGGCATCGCTACAAACAAGTACGTGGA C-3'	This study
narZ-del-R1	5'-CGGTGAGAGCAAATGACATGGCCATTGCC-3'	This study
narZ-del-F2	5'-CATGTCATTTGCTCTCACCCTCGCCGATG-3'	This study
narZ-del-R2	5'-GCATAAGGGAGAGCGCTTTTTTCGTACCAGGTGG CG-3'	This study

Table S3. Plasmids for bacterial mutant construction and gene complementation used in this study

Name	Description	References
pRDH10	<i>ori</i> (R6K) <i>mobRP4 sacRB</i> Tet ^R Cm ^R	(38)
pKD46	Spec ^R P _{BAD} - <i>gam-beta-exo oriR101 repA101^{ts}</i>	(39)
pKD3	Carb ^R FRT Cm ^R FRT PS1 PS2 <i>oriR6Kγ</i>	(39)
pKD13	Carb ^R FRT Kan ^R FRT PS1 PS4 <i>oriR6Kγ</i>	(39)
pBAD18	General expression vector with the P _{BAD} promoter, Kan ^R	(40)
pCAL61	pWSK129::□ cassette, Sm ^R , Kan ^R	(35)
pCAL62	pWSK29::□ cassette, Sm ^R , Carb ^R	(35)
pWJ43	pBAD18::P _{BAD} - <i>cutC</i>	This study
pWJ45	pRDH10:: $\Delta narG$	This study
pWJ46	pRDH10:: $\Delta napA$	This study
pWJ47	pRDH10:: $\Delta narZ$	This study

Table S4. Bacteria qPCR primers used in this study

Gene	Forward primer	Reverse primer
<i>cutN1</i>	5'-GGGTGATGCATTAGGGCTTA-3'	5'-TCGACAGATGCTTTCCTGC-3'
<i>cutC</i>	5'-AGCCTTGAGAACGCAGTGAT-3'	5'-CGTTGGATACGTGGTGTGTCAG-3'
<i>cutD</i>	5'-CACGGTCAGTGAATTGATGG-3'	5'-AACAGGAAGGTGTCGGTGAC-3'
<i>gyrB</i>	5'-GCAAAAAGCTGGAGCTGGTTA-3'	5'-CATTGGTGAAGGTTTCAAGG-3'

Table S5. Human qPCR primers used in this study

Gene	Forward primer	Reverse primer
<i>18S</i>	5'-GATATGCTCATGTGGTGTGGA-3'	5'-ACGTTCCACCTCATCCTCA-3'
<i>NDUFV1</i>	5'- CTGATCCCCAAGTCTGTGTGTGAGA -3'	5'-GATGTCCGTCGAGCGGTCCAT-3'
<i>NDUFS1</i>	5'- GAATGTGATCTGCAGGACCAGTC-3'	5'-GTCTTTACCAATGGCCCAATGT- 3'

Table S6. Mouse qPCR primers used in this study

Gene	Forward primer	Reverse primer
<i>β-actin</i>	5'-GCTGAGAGGGAAATCGTGCGTG-3'	5'-CCAGGGAGGAAGAGGATGCGG-3'
<i>Ndufv1</i>	5'-TTTCTCGGCGGGTTGGTTC-3'	5'-GGTTGGTAAAGATCCGGTCTTC-3'
<i>Ndufs1</i>	5'-AGGATATGTTTCGCACAACACTGG-3'	5'-TCATGGTAACAGAATCGAGGGA-3'
<i>Nos2</i>	5'-TTGGGTCTTGTTCACTCCACGG-3'	5'-CCTCTTTCAGGTCACTTTGGTAGG-3'

Table S7. Histopathology scoring criteria

Score	Inflammation	Epithelial proliferation
0	no inflammation	not present
1	Mild multifocal to diffuse accumulation of mononuclear cells and neutrophils in the lamina propria	Mild focal to multifocal enterocyte hyperplasia; mild loss of goblet cells; mild increase in mitotic figures (3-5 mitotic figures per 40x power field)
2	Moderate multifocal to diffuse accumulation of mononuclear cells and neutrophils in the lamina propria	Moderate focal to multifocal enterocyte hyperplasia; moderate loss of goblet cells; moderate increase in mitotic figures (6-9 mitotic figures per 40x power field)
3	Severe diffuse accumulation of mononuclear cells and neutrophils in the lamina propria	Severe multifocal to diffuse enterocyte hyperplasia; severe loss of goblet cells; severe increase in mitotic figures (>10 mitotic figures per 40x power field)

Table S8. Alcian blue scoring criteria

Score	Description
0	Absent alcian blue staining characterizing complete loss of goblet cells
1	Faint alcian blue staining characterizing marked to moderate multifocal to diffuse loss of goblet cells associated with low mucin content in the goblet cells still present
2	Moderate alcian blue staining characterizing mild multifocal to diffuse loss of goblet cells associated with intermediate mucin content in the goblet cells still present
3	Intense alcian blue staining characterizing adequate number of goblet cells associated with adequate mucin content in the goblet cells present (normal colonic mucosa)

Table S9. Product ions, declustering potential and collision energy parameters

Compound	DP	CE	Q1/Q3
<u>TMAO d9</u>	40	31	85/66
TMAO	40	31	76.1/58.1

References and Notes

1. A. Martínez-del Campo, S. Bodea, H. A. Hamer, J. A. Marks, H. J. Haiser, P. J. Turnbaugh, E. P. Balskus, Characterization and detection of a widely distributed gene cluster that predicts anaerobic choline utilization by human gut bacteria. *mBio* **6**, e00042–e15 (2015). [doi:10.1128/mBio.00042-15](https://doi.org/10.1128/mBio.00042-15) [Medline](#)
2. Z. Wang, E. Klipfell, B. J. Bennett, R. Koeth, B. S. Levison, B. Dugar, A. E. Feldstein, E. B. Britt, X. Fu, Y.-M. Chung, Y. Wu, P. Schauer, J. D. Smith, H. Allayee, W. H. W. Tang, J. A. DiDonato, A. J. Lusis, S. L. Hazen, Gut flora metabolism of phosphatidylcholine promotes cardiovascular disease. *Nature* **472**, 57–63 (2011). [doi:10.1038/nature09922](https://doi.org/10.1038/nature09922) [Medline](#)
3. Y. Zhu, E. Jameson, M. Crosatti, H. Schäfer, K. Rajakumar, T. D. H. Bugg, Y. Chen, Carnitine metabolism to trimethylamine by an unusual Rieske-type oxygenase from human microbiota. *Proc. Natl. Acad. Sci. U.S.A.* **111**, 4268–4273 (2014). [doi:10.1073/pnas.1316569111](https://doi.org/10.1073/pnas.1316569111) [Medline](#)
4. S. Devkota, Y. Wang, M. W. Musch, V. Leone, H. Fehlner-Peach, A. Nadimpalli, D. A. Antonopoulos, B. Jabri, E. B. Chang, Dietary-fat-induced taurocholic acid promotes pathobiont expansion and colitis in *Il10*^{-/-} mice. *Nature* **487**, 104–108 (2012). [doi:10.1038/nature11225](https://doi.org/10.1038/nature11225) [Medline](#)
5. N. Fei, L. Zhao, An opportunistic pathogen isolated from the gut of an obese human causes obesity in germfree mice. *ISME J.* **7**, 880–884 (2013). [doi:10.1038/ismej.2012.153](https://doi.org/10.1038/ismej.2012.153) [Medline](#)
6. M. Martinez-Medina, J. Denizot, N. Dreux, F. Robin, E. Billard, R. Bonnet, A. Darfeuille-Michaud, N. Barnich, Western diet induces dysbiosis with increased *E coli* in CEABAC10 mice, alters host barrier function favouring AIEC colonisation. *Gut* **63**, 116–124 (2014). [doi:10.1136/gutjnl-2012-304119](https://doi.org/10.1136/gutjnl-2012-304119) [Medline](#)
7. M. Anitha, F. Reichardt, S. Tabatabavakili, B. G. Nezami, B. Chassaing, S. Mwangi, M. Vijay-Kumar, A. Gewirtz, S. Srinivasan, Intestinal dysbiosis contributes to the delayed gastrointestinal transit in high-fat diet fed mice. *Cell. Mol. Gastroenterol. Hepatol.* **2**, 328–339 (2016). [doi:10.1016/j.jcmgh.2015.12.008](https://doi.org/10.1016/j.jcmgh.2015.12.008) [Medline](#)
8. P. A. Kakimoto, F. K. Tamaki, A. R. Cardoso, S. R. Marana, A. J. Kowaltowski, H₂O₂ release from the very long chain acyl-CoA dehydrogenase. *Redox Biol.* **4**, 375–380 (2015). [doi:10.1016/j.redox.2015.02.003](https://doi.org/10.1016/j.redox.2015.02.003) [Medline](#)
9. A. R. Cardoso, P. A. Kakimoto, A. J. Kowaltowski, Diet-sensitive sources of reactive oxygen species in liver mitochondria: Role of very long chain acyl-CoA dehydrogenases. *PLOS ONE* **8**, e77088 (2013). [doi:10.1371/journal.pone.0077088](https://doi.org/10.1371/journal.pone.0077088) [Medline](#)
10. C. J. Kelly, L. Zheng, E. L. Campbell, B. Saeedi, C. C. Scholz, A. J. Bayless, K. E. Wilson, L. E. Glover, D. J. Kominsky, A. Magnuson, T. L. Weir, S. F. Ehrentraut, C. Pickel, K. A. Kuhn, J. M. Lanis, V. Nguyen, C. T. Taylor, S. P. Colgan, Crosstalk between Microbiota-Derived Short-Chain Fatty Acids and Intestinal Epithelial HIF Augments Tissue Barrier Function. *Cell Host Microbe* **17**, 662–671 (2015). [doi:10.1016/j.chom.2015.03.005](https://doi.org/10.1016/j.chom.2015.03.005) [Medline](#)

11. Y. Litvak, M. X. Byndloss, A. J. Bäumlér, Colonocyte metabolism shapes the gut microbiota. *Science* **362**, eaat9076 (2018). [doi:10.1126/science.aat9076](https://doi.org/10.1126/science.aat9076) [Medline](#)
12. Y. Litvak, A. J. Bäumlér, Microbiota-Nourishing Immunity: A Guide to Understanding Our Microbial Self. *Immunity* **51**, 214–224 (2019). [doi:10.1016/j.immuni.2019.08.003](https://doi.org/10.1016/j.immuni.2019.08.003) [Medline](#)
13. C. R. Tiffany, A. J. Bäumlér, Dysbiosis: From fiction to function. *Am. J. Physiol. Gastrointest. Liver Physiol.* **317**, G602–G608 (2019). [doi:10.1152/ajpgi.00230.2019](https://doi.org/10.1152/ajpgi.00230.2019) [Medline](#)
14. M. X. Byndloss, E. E. Olsan, F. Rivera-Chávez, C. R. Tiffany, S. A. Cevallos, K. L. Lokken, T. P. Torres, A. J. Byndloss, F. Faber, Y. Gao, Y. Litvak, C. A. Lopez, G. Xu, E. Napoli, C. Giulivi, R. M. Tsohis, A. Revzin, C. B. Lebrilla, A. J. Bäumlér, Microbiota-activated PPAR- γ signaling inhibits dysbiotic Enterobacteriaceae expansion. *Science* **357**, 570–575 (2017). [doi:10.1126/science.aam9949](https://doi.org/10.1126/science.aam9949) [Medline](#)
15. E. M. Velazquez, H. Nguyen, K. T. Heasley, C. H. Saechao, L. M. Gil, A. W. L. Rogers, B. M. Miller, M. R. Rolston, C. A. Lopez, Y. Litvak, M. J. Liou, F. Faber, D. N. Bronner, C. R. Tiffany, M. X. Byndloss, A. J. Byndloss, A. J. Bäumlér, Endogenous Enterobacteriaceae underlie variation in susceptibility to Salmonella infection. *Nat. Microbiol.* **4**, 1057–1064 (2019). [doi:10.1038/s41564-019-0407-8](https://doi.org/10.1038/s41564-019-0407-8) [Medline](#)
16. A. Nissle, Weiteres über Grundlagen und Praxis der Mutaflorbehandlung. *DMW-Deutsche Medizinische Wochenschrift* **51**, 1809–1813 (1925). [doi:10.1055/s-0028-1137292](https://doi.org/10.1055/s-0028-1137292)
17. S. E. Winter, M. G. Winter, M. N. Xavier, P. Thiennimitr, V. Poon, A. M. Keestra, R. C. Laughlin, G. Gomez, J. Wu, S. D. Lawhon, I. E. Popova, S. J. Parikh, L. G. Adams, R. M. Tsohis, V. J. Stewart, A. J. Bäumlér, Host-derived nitrate boosts growth of *E. coli* in the inflamed gut. *Science* **339**, 708–711 (2013). [doi:10.1126/science.1232467](https://doi.org/10.1126/science.1232467) [Medline](#)
18. M. Gulhane, L. Murray, R. Lourie, H. Tong, Y. H. Sheng, R. Wang, A. Kang, V. Schreiber, K. Y. Wong, G. Magor, S. Denman, J. Begun, T. H. Florin, A. Perkins, P. Ó. Cuív, M. A. McGuckin, S. Z. Hasnain, High Fat Diets Induce Colonic Epithelial Cell Stress and Inflammation that is Reversed by IL-22. *Sci. Rep.* **6**, 28990 (2016). [doi:10.1038/srep28990](https://doi.org/10.1038/srep28990) [Medline](#)
19. N. Terada, N. Ohno, S. Saitoh, S. Ohno, Immunohistochemical detection of hypoxia in mouse liver tissues treated with pimonidazole using “in vivo cryotechnique”. *Histochem. Cell Biol.* **128**, 253–261 (2007). [doi:10.1007/s00418-007-0324-4](https://doi.org/10.1007/s00418-007-0324-4) [Medline](#)
20. S. Kizaka-Kondoh, H. Konse-Nagasawa, Significance of nitroimidazole compounds and hypoxia-inducible factor-1 for imaging tumor hypoxia. *Cancer Sci.* **100**, 1366–1373 (2009). [doi:10.1111/j.1349-7006.2009.01195.x](https://doi.org/10.1111/j.1349-7006.2009.01195.x) [Medline](#)
21. F. Rivera-Chávez, L. F. Zhang, F. Faber, C. A. Lopez, M. X. Byndloss, E. E. Olsan, G. Xu, E. M. Velazquez, C. B. Lebrilla, S. E. Winter, A. J. Bäumlér, Depletion of Butyrate-Producing Clostridia from the Gut Microbiota Drives an Aerobic Luminal Expansion of Salmonella. *Cell Host Microbe* **19**, 443–454 (2016). [doi:10.1016/j.chom.2016.03.004](https://doi.org/10.1016/j.chom.2016.03.004) [Medline](#)
22. C. A. Lopez, B. M. Miller, F. Rivera-Chávez, E. M. Velazquez, M. X. Byndloss, A. Chávez-Arroyo, K. L. Lokken, R. M. Tsohis, S. E. Winter, A. J. Bäumlér, Virulence factors

- enhance *Citrobacter rodentium* expansion through aerobic respiration. *Science* **353**, 1249–1253 (2016). [doi:10.1126/science.aag3042](https://doi.org/10.1126/science.aag3042) [Medline](#)
23. S. A. Cevallos, J.-Y. Lee, C. R. Tiffany, A. J. Byndloss, L. Johnston, M. X. Byndloss, A. J. Bäumlér, Increased Epithelial Oxygenation Links Colitis to an Expansion of Tumorigenic Bacteria. *mBio* **10**, e02244–e19 (2019). [doi:10.1128/mBio.02244-19](https://doi.org/10.1128/mBio.02244-19) [Medline](#)
 24. P. Thiennimitr, S. E. Winter, M. G. Winter, M. N. Xavier, V. Tolstikov, D. L. Huseby, T. Sterzenbach, R. M. Tsohis, J. R. Roth, A. J. Bäumlér, Intestinal inflammation allows *Salmonella* to use ethanolamine to compete with the microbiota. *Proc. Natl. Acad. Sci. U.S.A.* **108**, 17480–17485 (2011). [doi:10.1073/pnas.1107857108](https://doi.org/10.1073/pnas.1107857108) [Medline](#)
 25. F. Faber, P. Thiennimitr, L. Spiga, M. X. Byndloss, Y. Litvak, S. Lawhon, H. L. Andrews-Polymeris, S. E. Winter, A. J. Bäumlér, Respiration of Microbiota-Derived 1,2-propanediol Drives *Salmonella* Expansion during Colitis. *PLoS Pathog.* **13**, e1006129 (2017). [doi:10.1371/journal.ppat.1006129](https://doi.org/10.1371/journal.ppat.1006129) [Medline](#)
 26. S. Craciun, E. P. Balskus, Microbial conversion of choline to trimethylamine requires a glyceryl radical enzyme. *Proc. Natl. Acad. Sci. U.S.A.* **109**, 21307–21312 (2012). [doi:10.1073/pnas.1215689109](https://doi.org/10.1073/pnas.1215689109) [Medline](#)
 27. Z. Wang, A. B. Roberts, J. A. Buffa, B. S. Levison, W. Zhu, E. Org, X. Gu, Y. Huang, M. Zamanian-Daryoush, M. K. Culley, A. J. DiDonato, X. Fu, J. E. Hazen, D. Krajcik, J. A. DiDonato, A. J. Lusa, S. L. Hazen, Non-lethal Inhibition of Gut Microbial Trimethylamine Production for the Treatment of Atherosclerosis. *Cell* **163**, 1585–1595 (2015). [doi:10.1016/j.cell.2015.11.055](https://doi.org/10.1016/j.cell.2015.11.055) [Medline](#)
 28. C. Rousseaux, N. El-Jamal, M. Fumery, C. Dubuquoy, O. Romano, D. Chatelain, A. Langlois, B. Bertin, D. Buob, J. F. Colombel, A. Cortot, P. Desreumaux, L. Dubuquoy, The 5-aminosalicylic acid antineoplastic effect in the intestine is mediated by PPAR γ . *Carcinogenesis* **34**, 2580–2586 (2013). [doi:10.1093/carcin/bgt245](https://doi.org/10.1093/carcin/bgt245) [Medline](#)
 29. S. A. Cevallos, J.-Y. Lee, E. M. Velazquez, N. J. Foegeding, C. D. Shelton, C. R. Tiffany, B. H. Parry, A. R. Stull-Lane, E. E. Olsan, H. P. Savage, H. Nguyen, S. S. Ghanaat, A. J. Byndloss, I. O. Agu, R. M. Tsohis, M. X. Byndloss, A. J. Bäumlér, 5-Aminosalicylic Acid Ameliorates Colitis and Checks Dysbiotic *Escherichia coli* Expansion by Activating PPAR- γ Signaling in the Intestinal Epithelium. *mBio* **12**, e03227–e20 (2021). [doi:10.1128/mBio.03227-20](https://doi.org/10.1128/mBio.03227-20) [Medline](#)
 30. G. G. Schiattarella, A. Sannino, E. Toscano, G. Giugliano, G. Gargiulo, A. Franzone, B. Trimarco, G. Esposito, C. Perrino, Gut microbe-generated metabolite trimethylamine-N-oxide as cardiovascular risk biomarker: A systematic review and dose-response meta-analysis. *Eur. Heart J.* **38**, 2948–2956 (2017). [doi:10.1093/eurheartj/ehx342](https://doi.org/10.1093/eurheartj/ehx342) [Medline](#)
 31. S. Nishikawa, A. Yasoshima, K. Doi, H. Nakayama, K. Uetsuka, Involvement of sex, strain and age factors in high fat diet-induced obesity in C57BL/6J and BALB/cA mice. *Exp. Anim.* **56**, 263–272 (2007). [doi:10.1538/expanim.56.263](https://doi.org/10.1538/expanim.56.263) [Medline](#)
 32. C. Gallou-Kabani, A. Vigé, M.-S. Gross, J.-P. Rabès, C. Boileau, C. Larue-Achagiotis, D. Tomé, J.-P. Jais, C. Junien, C57BL/6J and A/J mice fed a high-fat diet delineate components of metabolic syndrome. *Obesity* **15**, 1996–2005 (2007). [doi:10.1038/oby.2007.238](https://doi.org/10.1038/oby.2007.238) [Medline](#)

33. U. S. Pettersson, T. B. Waldén, P. O. Carlsson, L. Jansson, M. Phillipson, Female mice are protected against high-fat diet induced metabolic syndrome and increase the regulatory T cell population in adipose tissue. *PLOS ONE* **7**, e46057 (2012). [doi:10.1371/journal.pone.0046057](https://doi.org/10.1371/journal.pone.0046057) [Medline](#)
34. J. G. Falls, B. L. Blake, Y. Cao, P. E. Levi, E. Hodgson, Gender differences in hepatic expression of flavin-containing monooxygenase isoforms (FMO1, FMO3, and FMO5) in mice. *J. Biochem. Toxicol.* **10**, 171–177 (1995). [doi:10.1002/jbt.2570100308](https://doi.org/10.1002/jbt.2570100308) [Medline](#)
35. A. M. Spees, T. Wangdi, C. A. Lopez, D. D. Kingsbury, M. N. Xavier, S. E. Winter, R. M. Tsolis, A. J. Bäumlér, Streptomycin-induced inflammation enhances *Escherichia coli* gut colonization through nitrate respiration. *mBio* **4**, e00430–e13 (2013). [doi:10.1128/mBio.00430-13](https://doi.org/10.1128/mBio.00430-13) [Medline](#)
36. R. Simon, U. Prierer, A. Puhler, A Broad Host Range Mobilization System for In vivo Genetic-Engineering - Transposon Mutagenesis in Gram-Negative Bacteria. *Biotechnology* **1**, 784–791 (1983). [doi:10.1038/nbt1183-784](https://doi.org/10.1038/nbt1183-784)
37. J. Xu, M. K. Bjursell, J. Himrod, S. Deng, L. K. Carmichael, H. C. Chiang, L. V. Hooper, J. I. Gordon, A genomic view of the human-Bacteroides thetaiotaomicron symbiosis. *Science* **299**, 2074–2076 (2003). [doi:10.1126/science.1080029](https://doi.org/10.1126/science.1080029) [Medline](#)
38. R. A. Kingsley, R. Reissbrodt, W. Rabsch, J. M. Ketley, R. M. Tsolis, P. Everest, G. Dougan, A. J. Bäumlér, M. Roberts, P. H. Williams, Ferrioxamine-mediated Iron(III) utilization by *Salmonella enterica*. *Appl. Environ. Microbiol.* **65**, 1610–1618 (1999). [doi:10.1128/AEM.65.4.1610-1618.1999](https://doi.org/10.1128/AEM.65.4.1610-1618.1999) [Medline](#)
39. K. A. Datsenko, B. L. Wanner, One-step inactivation of chromosomal genes in *Escherichia coli* K-12 using PCR products. *Proc. Natl. Acad. Sci. U.S.A.* **97**, 6640–6645 (2000). [doi:10.1073/pnas.120163297](https://doi.org/10.1073/pnas.120163297) [Medline](#)
40. L. M. Guzman, D. Belin, M. J. Carson, J. Beckwith, Tight regulation, modulation, and high-level expression by vectors containing the arabinose PBAD promoter. *J. Bacteriol.* **177**, 4121–4130 (1995). [doi:10.1128/jb.177.14.4121-4130.1995](https://doi.org/10.1128/jb.177.14.4121-4130.1995) [Medline](#)